

Asymmetric Jump Processes: Option Pricing Implications

Brice Dupoyet *

June 10, 2004

Abstract

This article proposes and tests a convenient, easy to use closed-form solution for the pricing of a European Call option where the underlying asset is subject to upward and downward jumps displaying separate distributions and probabilities of occurrence. The setup presented in this article lays in contrast to the assumption of lognormality in the jump magnitude generally made in the option pricing literature and can be used by academics and practitioners alike as it allows for a more precise modeling of the implied volatility smile. Through the use of both simulations and actual options data on the S&P 500 index it is shown that the asymmetric jump model captures deviations from the standard geometric Brownian motion with more precision than the lognormal jump setup is able to achieve.

* Corresponding author: Brice Dupoyet, Florida International University, College of Business Administration, University Park, RB 209A, Miami, FL 33199, phone (305) 348 3328, e-mail dupoyetb@fiu.edu

It is a well-established fact that when volatility levels are inferred from observed option prices using the Black-Scholes option pricing formula and plotted against the exercise price, an implied “volatility smile” or “smirk” is ubiquitously observed in both stock and currency markets as demonstrated by Ball and Torous [1983, 1985], Jorion [1988], Bakshi, Cao, and Chen [1997], Bates [1988, 1991, 1996, 2000], Doffou and Hilliard [2001] or Pan [2002] to only name a few.

The excess kurtosis and skewness causing this smile is present in the implied transition density function of most securities’ observed rates of return and can be partially explained through the modeling of jumps but also through the use of stochastic volatility (Heston, [1993]) or both as shown in Scott [1997], Bakshi et al. [1997], Pan [2002], or Eraker, Johannes, and Polson [2003]. Stochastic volatility usually has a larger impact on long term options whereas the presence of jumps mostly benefits the pricing of short term near-the-money options. A combination of the two features thus generally explains the shape of the smile and the distribution of returns better than the simpler jump-diffusion model. However, stochastic volatility is not considered here in order to focus on the effects of jumps alone, although a solution incorporating this feature could still be obtained in the same fashion. This paper concentrates on relaxing the traditional assumption of a common lognormal jump distribution spanning both upward and downward jumps by allowing each jump type to possess distinct distributional properties.

Since the seminal work of Merton [1976], the notion that allowing for jumps in a security’s rate of return improves the modeling of the so-called “implied volatility smile” has been widely accepted by academics and practitioners everywhere. The traditional lognormality assumption involves a “generic jump” whose magnitude fluctuates between minus one and infinity, thus allowing the generation of both downward and upward jumps. Although the lognormal distribution has many useful properties, one drawback of this approach is the constraining of upward jumps and downward jumps to both come from the same distribution as well as the lack of precise differentiation between the probabilities of occurrence of each type of jump. This is in part because in the lognormal setup the Poisson process determining whether a jump occurs and the jump magnitude -and therefore type- are assumed to be two independent processes. In addition, the jump magnitude expected should a downward jump occur could potentially be very different from the magnitude expected should an upward one

take place instead. It would thus seem natural to wish to allow for that higher level of flexibility by allowing the jump magnitude to be conditional on the jump type.

Ramezani and Zeng [1999] conduct a Maximum Likelihood Estimation on security prices allowing for two types of jumps, focusing directly on times series of stock returns. They show that allowing for a mixture of distribution for the up-jumps and down-jumps proves to be a better fit to the data than having a common distribution spawning both. Securities thus seem to behave more in accordance with a dual jump distribution setup than the assumed lognormal function. Investigating the implication of this finding in the pricing of options therefore seems to be the next logical step.

I. THE MODEL

The model used to derive the solution to the European call option pricing problem can be found in Ramezani and Zeng [1999], Kou and Wang [2001] and Kou [2002]. Let $S(t)$ represent the value of the underlying asset at time t paying a constant continuous dividend yield q , and assume that the instantaneous return on the asset is determined by the following risk-neutral process:

$$\frac{dS(t)}{S(t)} = (R - q - \frac{\lambda_u}{r_u - 1} + \frac{\lambda_d}{r_d + 1})dt + \sigma dW(t) + J_u(t)dq_u(t) + J_d(t)dq_d(t) \quad (1)$$

where

- R and q are the instantaneous interest rate and dividend yield;
- λ_u and λ_d are the frequency of upward jumps and downward jumps per year;
- $J_u(t)$ is the percentage up-jump size conditionally on an upward jump occurring defined as: $J_u(t) = x_u(t) - 1$ with $x_u(t)$ distributed $Pareto(r_u)$;
- $J_d(t)$ is the percentage down-jump size conditionally on a downward jump occurring defined as: $J_d(t) = x_d(t) - 1$ with $x_d(t)$ distributed $Beta(r_d, 1)$;
- σ is the diffusion component of the return variance conditional on no jumps occurring;
- $W(t)$ is a standard Brownian motion;
- $q_u(t)$ and $q_d(t)$ are Poisson up and down jump counters with intensities λ_u and λ_d .

The Pareto and Beta density functions for the up-jump and down-jump magnitudes are assumed to follow:

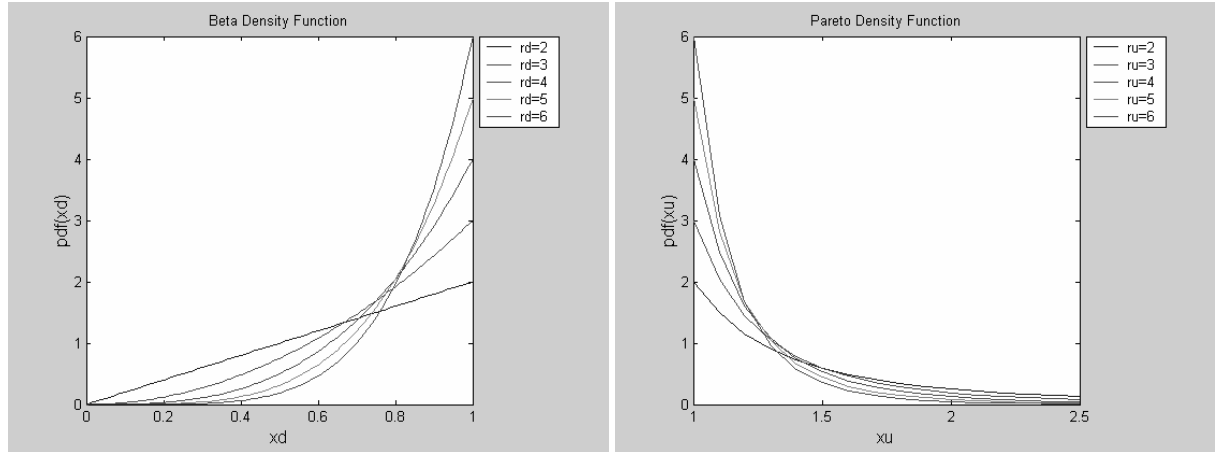
$$f_{x_u}(x_u) = r_u \left(\frac{1}{x_u} \right)^{r_u+1} \text{ with } x_u \geq 1 \text{ and } E(x_u) = \frac{r_u}{r_u - 1} \text{ and } \sigma_{x_u}^2 = \frac{r_u}{(r_u - 2)(r_u - 1)^2}$$

$$f_{x_d}(x_d) = r_d (x_d)^{r_d-1} \text{ with } 0 < x_d < 1 \text{ and } E(x_d) = \frac{r_d}{r_d + 1} \text{ and } \sigma_{x_d}^2 = \frac{r_d}{(r_d + 2)(r_d + 1)^2}$$

By varying the parameters r_u and r_d the shapes of the Beta and Pareto probability distribution functions can be calibrated for the downward and upward jumps as shown in the following Exhibit.

EXHIBIT 1

Evolution of the Beta and Pareto probability density functions with r_d and r_u



II. SOLUTION

With two different types of jumps present, the European call option must satisfy the following partial differential equation:

$$-\frac{\partial C}{\partial \tau} + \left(R - q - \frac{\lambda_u}{r_u - 1} + \frac{\lambda_d}{r_d + 1} \right) S \frac{\partial C}{\partial S} + \frac{1}{2} \sigma^2 S^2 \frac{\partial^2 C}{\partial S^2} - RC + \lambda_u E^Q \{ C(S(1 + J_u)) - C(S) \} + \lambda_d E^Q \{ C(S(1 + J_d)) - C(S) \} = 0 \quad (2)$$

Solving equation (2) in the appendix, the price of a European call option on an asset displaying the dynamics specified in equation (1) is

$$C(t, \tau) = S(t)e^{-q\tau}\Pi_1(t, \tau, S) - Ke^{-R\tau}\Pi_2(t, \tau, S)$$

with

$$\Pi_j(t, \tau, S) = \frac{1}{2} + \frac{1}{\pi} \int_0^{\infty} \operatorname{Re} \left[\frac{e^{-i\phi \ln(K)} f_j(t, \tau, S, \phi)}{i\phi} \right] d\phi \quad \text{for } j = 1, 2 \quad (3)$$

where explicit solutions to the characteristic functions f_1 and f_2 are derived in the appendix.

III. SIMULATIONS

To first demonstrate the flexibility of the model, simulations of implied volatility smiles are performed. The idea is to examine what shapes the smile is able to take provided that the underlying asset abides by the dynamics specified in the section II, for some given parameters. The procedure is as follows. First, some model parameters are arbitrarily selected and used as inputs in the call option pricing formula derived in the previous section. This step includes selecting a volatility level, frequency and magnitude of upward and downward jumps, time to maturity and a risk-free rate. Second, various option prices are generated using the formula by letting the spot-to-exercise price ratio vary. Third, implied volatility levels are inferred from each option price generated in the previous step using this time the Black-Scholes option pricing formula instead. This third step creates a series of implied volatility levels corresponding to various moneyness levels. The familiar volatility smile is finally obtained by plotting the volatility values against moneyness levels.

Hence this smile is what would be observed in the market if the underlying asset did exactly follow the dynamics specified in equation (1). In order to establish the impact of a given variable, additional smiles are generated by repeating the process for each variable, with results shown in Exhibits 2 and 3. The jump-related parameters selected for the simulation are $\lambda_u = 0.2$, $\lambda_d = 0.2$, $r_u = 5$, and $r_d = 5$, with a domestic risk-free rate set to 5% and no dividend yield, implying a potential downward jump with a mean of -16.67% and a potential upward jump with a mean of 25%.

EXHIBIT 2

Evolution of the implied volatility smile with λ_d and λ_u

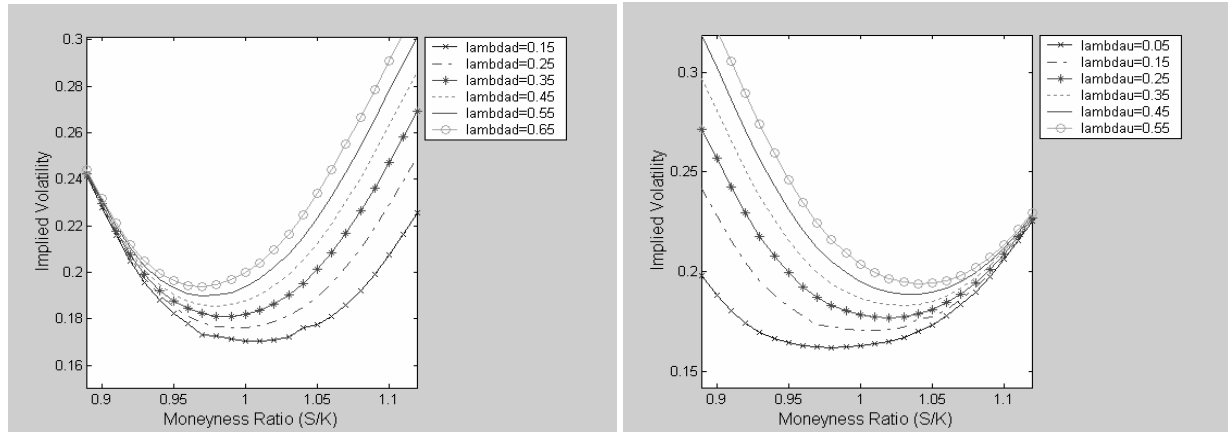
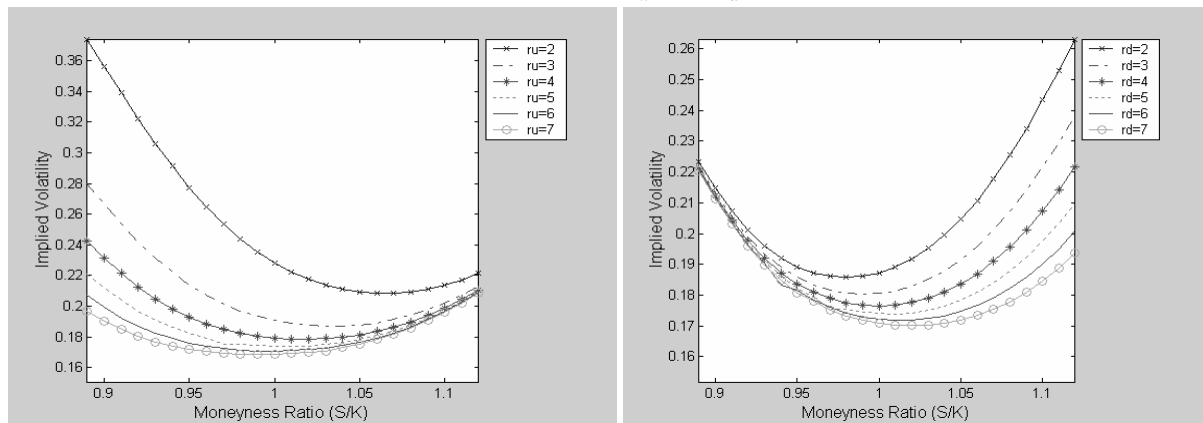


EXHIBIT 3

Evolution of the implied volatility smile with r_u and r_d



The simulations show that using the appropriate combination of parameters, the asymmetric jump model should be able to easily replicate smiles taking almost any shape. The smile can be flattened, made steeper, or steep at one end and flatter at the other. Through these simulations at least, the model appears relatively flexible. The next step is thus to evaluate its pricing abilities on actual data. In order to demonstrate the benefits of using a more sophisticated modeling of jumps in the security's rates of return, the lognormal and asymmetric jumps models are estimated and compared on actual S&P 500 European options data in the next section.

IV. ESTIMATION AND COMPARISON PROCEDURE

The data used for the model comparison consist of end-of-the-day European call option prices on the S&P 500 index from January 2001 to December 2002. The SPX information is obtained from the CBOE exchange, for a total number of 151,991 records. For each day the last options quotes of the day and moneyness are collected across maturities along with the corresponding value of the index. The LIBOR rate is selected as the risk-free rate proxy with maturities matching the maturities of the options. When the LIBOR maturity does not exactly coincide with the option expiration date, the appropriate risk-free rate is computed by interpolating between the closest two LIBOR rates straddling the desired period.

Since the models under scrutiny do not incorporate stochastic volatility it is deemed more appropriate to compare the lognormal jump model and the asymmetric jump model on a specific day as opposed to a week or a month. The implicit assumption is that even if the volatility is stochastic, its level is relatively constant during a fraction of a day. In order to establish how the models fare in various market conditions, VIX levels are examined to select months of high, low, and average levels of volatility in the spirit of Pan [2002]. Within these months, days are randomly selected as an attempt to represent fairly various possible states of the market. Differences in the models' performances will be identified by the closeness of a given model's implied volatility smile to the observed prices' implied volatility smile. A model that prices options perfectly would display an implied volatility smile that exactly describes the Black-Scholes implied volatility smile obtained from observed prices.

The estimation and evaluation procedure for each model is as follows. For a given day a cross section of closing option prices of a given maturity is recorded. The focus is on options of relatively short maturity as these options tend to display the deepest smiles and are the ones for which the introduction of jumps makes the largest pricing improvement, as the contribution of jumps is known to decline with a longer option maturity. Options of 20 to 30 days to maturity are therefore selected and the cross-sectional dataset is used to estimate the model parameters using the information embedded in option market prices across the various moneyness levels. Let $C_n(t, S, \tau_n, R, q, K_n)$ be the observed option price on the n^{th} option in the sample on day t , let $\hat{C}_n(t, S, \tau_n, R, q, K_n)$ be the model-driven option price given a set of parameters Θ and a volatility

level σ , let K_n and τ_n be the exercise price and time-to-maturity of that n^{th} option, let R and q be respectively the risk-free rate and dividend yield on day t and let S be the value of the spot index on that same day. For the estimation of the parameters a generalized least square procedure is performed where the function to be minimized on day t is

$$\mathit{Min}_{\sigma, \Theta} \sum_{n=1}^N \left[C_n(t, S, \tau_n, R, q, K_n) - \hat{C}_n(t, S, \tau_n, R, q, K_n) \right]^2 \quad (4)$$

Note that the volatility σ is estimated along with the rest of the model parameters Θ and is therefore treated as such.

EXHIBIT 4
Monthly VIX levels for 2001 and 2002

Month	2001	2002
January	24.92	22.22
February	23.48	22.88
March	28.50	18.99
April	28.34	19.90
May	22.94	20.09
June	20.94	25.27
July	22.32	34.05
August	21.83	33.74
September	35.07	37.65
October	32.72	35.24
November	26.68	28.10
December	23.72	28.21

Once the parameters are estimated they are used to compute one day-ahead out-of-sample model-predicted option prices for each moneyness level by plugging in the parameters and the observed variables – such as the index level, the dividend yield, the LIBOR rate, the exercise price and the time to maturity - into the respective models for the following day. Finally, implied volatility levels are inferred from the model using the Black Scholes formula on the model-predicted prices as well as on the observed option prices for comparison. If the model is an exact description of reality, the market observed option prices' implied volatility smile and the model-predicted option prices' implied volatility smile should be the same.

Monthly VIX levels for the year 2001 and 2002 are displayed in Exhibit 4. In 2001, June, September and November are months of low, high and average volatility respectively. In 2002, March, September and November are months of low, high and average volatility respectively. In order to account for various possible states of the market, six days are randomly chosen that belong to these six months for purposes of testing the performance of the lognormal and asymmetric jump option pricing models.

V. RESULTS

The implied volatility plots comparing the lognormal and asymmetric jump models are displayed in Exhibits 5 through 7. The “Black Scholes model” curve represents Black-Scholes implied volatility levels inferred from actual (observed) option prices, whereas the curves titled “lognormal model” and “asymmetric jump model” represent Black-Scholes implied volatility levels inferred from theoretically-computed option prices. The theoretical option prices are obtained using the asymmetric jump call option pricing formula derived earlier as well as the traditional lognormal jump call option pricing formula, along with the respective corresponding parameters estimated on the previous day.

Overall the results are fairly consistent across periods of different volatility levels. For out-of-the-money and at-the-money options the performances of the lognormal jump and the asymmetric jump model are nearly identical. However, in the case of out-of-the-money options the asymmetric jump model captures the shape of the smile more accurately as its implied

volatility smile is visually much closer to the observed option prices' volatility smile than the lognormal jump model. By using the asymmetric jump model instead of the traditional lognormal jump model one can therefore better replicate the implied volatility smile for some moneyness range.

EXHIBIT 5
Implied Volatility Smiles on days in low-volatility months

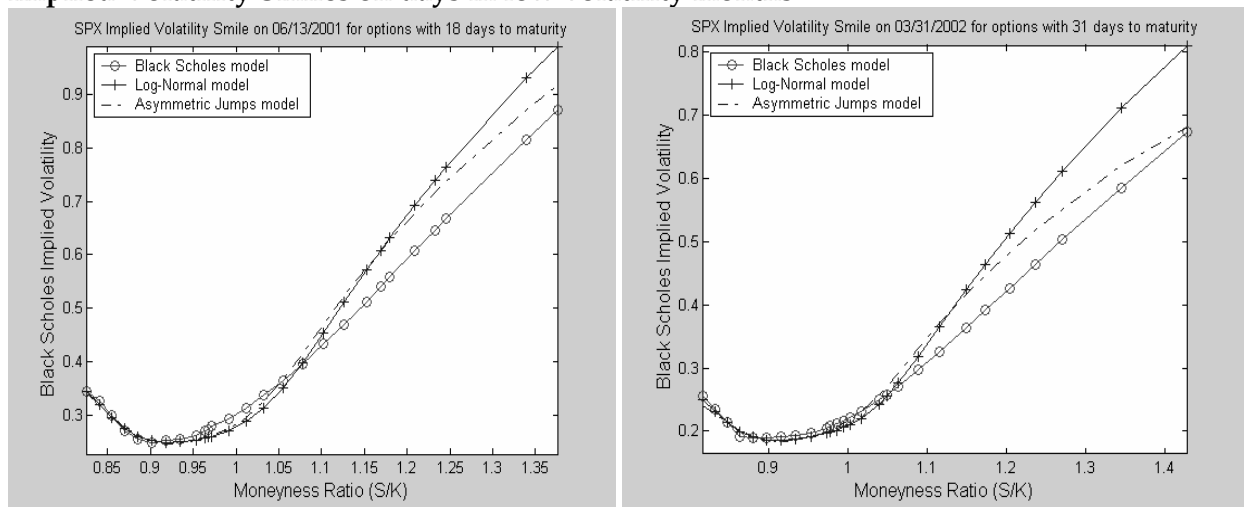


EXHIBIT 6
Implied Volatility Smiles on days in medium-volatility months

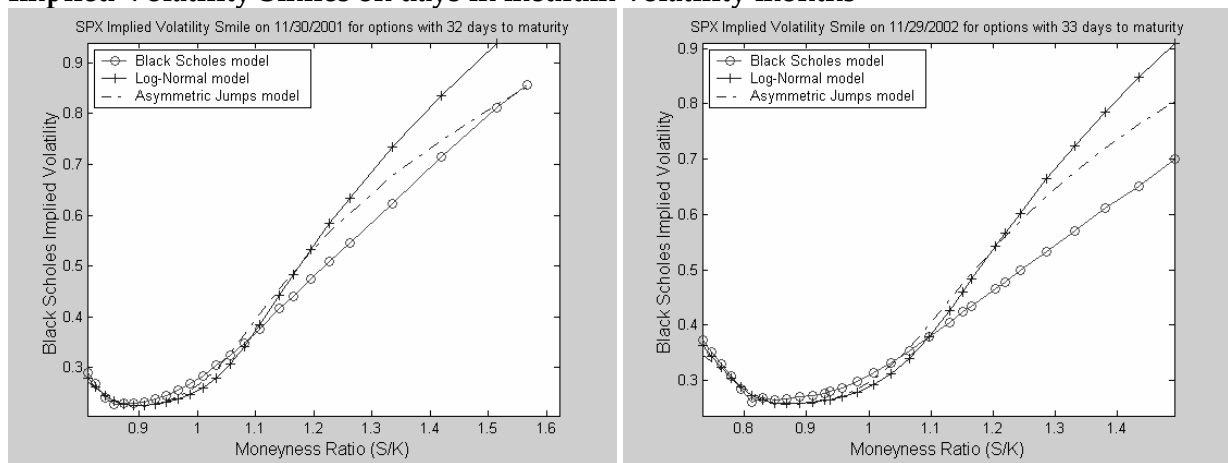
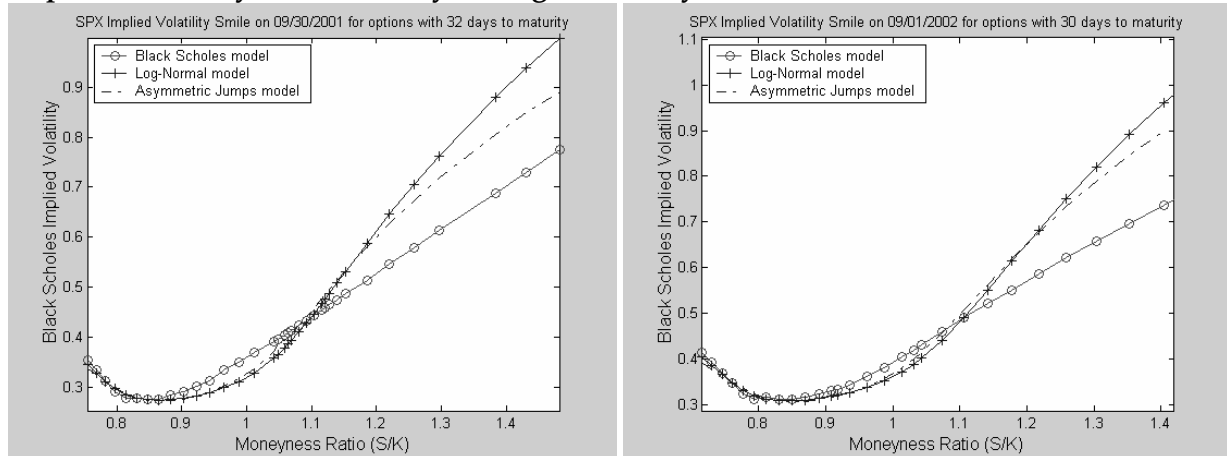


EXHIBIT 7

Implied Volatility Smiles on days in high-volatility months



An explanation for this observation may be that while the lognormal jump model is able to capture the smile in the out-of-the-money range, it can only do so by calibrating the model's parameters in a way that implies a non-negligible chance of a positive jump. That same positive jump helping the model in the out-of-the-money range can then hurt the model in the in-the-money range if the setup does not have the ability to offset the positive jump effect with a distinct downward jump probability and magnitude. This inability to decrease option prices in the in-the-money range creates an implied volatility smile that lays too high in value. The asymmetric jump model is on the other hand able to decrease option prices in the in-the-money range while maintaining a good fit in the out-of-the money range thanks to the independent and precise likelihood of a downward jump. Decreasing model-predicted option values in the in-the-money range translates into a lower smile in that range, hence a smile that is closer to the observed volatility smile for options whose moneyness is above one.

Since implied volatility plots are not as important as Dollar amounts we may want to ask what some of these results translate into financially. For example, for a European call option with an exercise price of \$900, a spot index level of 1258, a risk-free rate of 6%, a dividend yield of 2% and 30 days to maturity, a 10% difference in volatility levels will roughly translate into a \$2 per unit price differential, or \$200 per contract. Note that this number can be even larger for some of the even deeper in-the-money cases observed on the graphs. When holding a large quantity of contracts, the impact of the pricing differential can thus become highly significant.

Finally, note that although this study concentrates on a case of constant volatility in order to focus on the contribution of jumps alone, it is also possible to integrate stochastic volatility into the dynamics of the process in equation (1). Incorporating additional features such as stochastic volatility is not being considered here as this paper focuses on the marginal benefits of modeling jumps in a more flexible manner. Although the constant volatility assumption may seem restrictive, the goal of the paper is not to identify the most general model possible, but rather to focus on one specific feature dear to option pricing theorists and demonstrate through the use of simulations and empirical testing that it can be taken to a new level.

The pricing abilities of a model incorporating stochastic volatility and jumps would doubtlessly improve even further as asymmetric jumps are introduced in the setup, as demonstrated in this paper for the constant volatility case.

VI. CONCLUSION

A new setup improving the modeling of jumps in equity and currency returns is presented. Replacing the traditional lognormal distribution for the jump magnitude, the Beta and Pareto distributions are convenient to work with as the ranges of their respective random variables precisely meet the requirements of upward and downward jump magnitudes. The model is fairly easy to use as a closed-form solution is obtained for the pricing of European call options despite a more complex description of the security's rate of return jump dynamics.

Out-of-sample tests show that using a combination of Pareto and Beta distributions leads to a more accurate modeling of the implied volatility smile than the traditional lognormal setup and thus to a more accurate pricing of the options. More generally, this new paradigm can benefit any option pricing model that already incorporates jumps in the underlying process but uses a lognormality assumption to describe the jump magnitude.

APPENDIX A

Derivation of European Call Option in Double-Jump Setting

By standard argument, the European call option must satisfy the following pde:

$$-\frac{\partial C}{\partial \tau} + \left(R - q - \frac{\lambda_u}{r_u - 1} + \frac{\lambda_d}{r_d + 1} \right) S \frac{\partial C}{\partial S} + \frac{1}{2} \sigma^2 S^2 \frac{\partial^2 C}{\partial S^2} - RC + \lambda_u E^Q \{ C(S(1 + J_u)) - C(S) \} + \lambda_d E^Q \{ C(S(1 + J_d)) - C(S) \} = 0 \quad (\text{A-1})$$

Applying the transformation $L(t) = \ln[S(t)]$ yields:

$$-\frac{\partial C}{\partial \tau} + \left(R - q - \frac{\lambda_u}{r_u - 1} + \frac{\lambda_d}{r_d + 1} - \frac{1}{2} \sigma^2 \right) \frac{\partial C}{\partial L} + \frac{1}{2} \sigma^2 \frac{\partial^2 C}{\partial L^2} - RC + \lambda_u E^Q \{ C(L + \ln(x_u)) - C(L) \} + \lambda_d E^Q \{ C(L + \ln(x_d)) - C(L) \} = 0 \quad (\text{A-2})$$

Conjecture that $C(t, \tau) = S(t) e^{-q\tau} \Pi_1(t, \tau, S) - K e^{-R\tau} \Pi_2(t, \tau, S)$. Plugging this form into (A-2) produces the Fokker-Planck forward equations for the risk-neutral probabilities Π_1 and Π_2 also satisfied by the respective characteristic functions as shown by Heston [1993]:

$$-\frac{\partial f_1}{\partial \tau} + \left(R - q - \frac{\lambda_u}{r_u - 1} + \frac{\lambda_d}{r_d + 1} + \frac{1}{2} \sigma^2 \right) \frac{\partial f_1}{\partial L} + \frac{1}{2} \sigma^2 \frac{\partial^2 f_1}{\partial L^2} + \left(-\frac{\lambda_u}{r_u - 1} + \frac{\lambda_d}{r_d + 1} \right) f_1 + \lambda_u E^Q \{ x_u f_1(L + \ln(x_u)) - f_1(L) \} + \lambda_d E^Q \{ x_d f_1(L + \ln(x_d)) - f_1(L) \} = 0 \quad (\text{A-3})$$

$$-\frac{\partial f_2}{\partial \tau} + \left(R - q - \frac{\lambda_u}{r_u - 1} + \frac{\lambda_d}{r_d + 1} - \frac{1}{2} \sigma^2 \right) \frac{\partial f_2}{\partial L} + \frac{1}{2} \sigma^2 \frac{\partial^2 f_2}{\partial L^2} + \lambda_u E^Q \{ f_2(L + \ln(x_u)) - f_2(L) \} + \lambda_d E^Q \{ f_2(L + \ln(x_d)) - f_2(L) \} = 0 \quad (\text{A-4})$$

with boundary conditions $f_1 = e^{i\phi \ln(S)}$ and $f_2 = e^{i\phi \ln(S)}$ at expiration.

Conjecture that the solutions to (A-3) and (A-4) are of the following forms:

$$f_1(t, \tau, S, \phi) = e^{\alpha(\tau) + i\phi L} \quad \text{and} \quad f_2(t, \tau, S, \phi) = e^{\beta(\tau) + i\phi L} \quad \text{with} \quad \alpha(0) = \beta(0) = 0 \quad (\text{A-5})$$

Plugging these solutions into (A-3) and (A-4) and making use of the distributional assumptions for the magnitude of the up-jumps and down-jumps yields the following solutions:

$$f_1(t, \tau, S, \phi) = \exp \left\{ -\frac{1}{2} \sigma^2 \phi^2 \tau + i\phi \left(R - q - \frac{\lambda_u}{r_u - 1} + \frac{\lambda_d}{r_d + 1} + \frac{1}{2} \sigma^2 \right) \tau + \frac{\lambda_d}{r_d + 1} \tau - \frac{\lambda_u}{r_u - 1} \tau \right. \\ \left. + \frac{\lambda_u r_u}{r_u - i\phi - 1} \tau + \frac{\lambda_d r_d}{r_d + i\phi + 1} \tau - (\lambda_u + \lambda_d) \tau + i\phi \ln(S) \right\} \quad (\text{A-6})$$

$$f_2(t, \tau, S, \phi) = \exp \left\{ -\frac{1}{2} \sigma^2 \phi^2 \tau + i\phi \left(R - q - \frac{\lambda_u}{r_u - 1} + \frac{\lambda_d}{r_d + 1} - \frac{1}{2} \sigma^2 \right) \tau \right. \\ \left. + \frac{\lambda_u r_u}{r_u - i\phi} \tau + \frac{\lambda_d r_d}{r_d + i\phi} \tau - (\lambda_u + \lambda_d) \tau + i\phi \ln(S) \right\} \quad (\text{A-7})$$

with Π_1 and Π_2 recovered from f_1 and f_2 by Fourier inversion.

Q.E.D.

REFERENCES

- Ball, C., and W. Torous. "A Simplified Jump Process for Common Stock Returns." *Journal of Financial and Quantitative Analysis*, 18 (1983), pp. 53-65.
- Ball, C., and W. Torous. "On Jumps in Common Stock Prices and Their Impact on Call Option Pricing." *Journal of Finance*, 40 (1985), pp. 155-173.
- Bakshi, G., C. Cao, and Z. Chen. "Empirical Performance of Alternative Option Pricing Models." *Journal of Finance*, 52 (1997), pp. 2003-2049.
- Bates, D. "Pricing Options Under Jump-Diffusion Processes." University of Iowa Working Paper, 1-28, 1988.
- Bates, D. "The Crash of '87: Was It Expected? The Evidence from Options Markets." *Journal of Finance*, 46 (1991), pp. 1009-1044.
- Bates, D. "Jumps and Stochastic Volatility: Exchange Rate Processes Implicit in Deutsche Mark Options." *Review of Financial Studies*, 9 (1996), pp. 69-107.
- Bates, D. "Dollar Jump Fears, 1984-1992: Distributional Abnormalities Implicit in Currency Futures Options." *Journal of International Money and Finance*, 15 (1996), pp. 65-93.
- Bates, D. "Post-'87 Crash Fears in the S&P 500 Futures Option Market." *Journal of Econometrics*, 94 (2000), pp. 181-238.
- Black, F., and M. Scholes. "The Pricing of Options and Corporate Liabilities." *Journal of Political Economy*, 81 (1973), pp. 637-659.
- Doffou, A., and J. Hilliard. "Pricing Currency Options Under Stochastic Interest Rates and Jump-Diffusion Processes." *The Journal of Financial Research*, 24 (2001), pp. 565-585.
- Eraker, B., M. Johannes, and N. Polson. "The Impact of Jumps in Volatility and Returns." *Journal of Finance*, 58 (2003), pp. 1269-1300.
- Heston, S. "A Closed-Form Solution for Options with Stochastic Volatility with Applications to Bond and Currency Options." *The Review of Financial Studies*, 6 (1993), pp. 327-343.
- Jorion, P. "On Jump Processes in the Foreign Exchange and Stock Markets." *The Review of Financial Studies*, 1 (1988), pp. 427-445.
- Kou, S. "A Jump-Diffusion Model for Option Pricing." *Management Science*, 48(8) (2002), pp. 1086-1101.

Kou, S., and H. Wang. "Option Pricing Under a Double Exponential Jump Diffusion Model." Working Paper, 2001.

Merton, R. "Option Pricing When Underlying Stock Returns Are Discontinuous." *Journal of Financial Economics*, 3 (1976), pp. 125-144.

Pan, J. "The Jump-Risk Premia Implicit in Options: Evidence from an Integrated Time-Series Study." *Journal of Financial Economics*, 63 (2002), pp. 3-50.

Ramezani, C., and Y. Zeng. "Maximum Likelihood Estimation of Asymmetric Jump-Diffusion Processes: Application to Security Prices." Working Paper, 1999.

Scott, L. "Pricing Stock Options in a Jump-Diffusion Model with Stochastic Volatility and Interest Rates: Applications of Fourier Inversion Methods." *Mathematical Finance*, 7 (1997), pp. 413-424.